

Article

Design and Implementation of a 16-Electrode Electrical Impedance Tomography Data Acquisition System for Medical Imaging

Aldo Nofrianto^{1*}, Audy², and Aditya Wardani³,¹⁻³ Politeknik Negeri Padang, Padang, Indonesia

* Correspondence: aldonofrianto@pnp.ac.id

Received: 24 December 2025; Revised: 29 December 2025; Accepted: 30 December 2025; Published: 31 December 2025

Abstract: Electrical Impedance Tomography (EIT) requires a stable and accurate data acquisition system to obtain reliable boundary voltage measurements for medical imaging applications. However, many existing EIT systems are complex and costly, limiting their practical use in clinical and research environments. This paper presents the design, implementation, and experimental validation of a 16-electrode EIT data acquisition system for medical imaging. The proposed system consists of a sinusoidal signal generator, voltage-to-current converter (VCC), voltage measurement circuit, multiplexer/demultiplexer unit, microcontroller, and image reconstruction algorithm. Experimental evaluations were conducted to assess signal stability, current injection performance, and voltage measurement accuracy. The XR2206-based signal generator demonstrated stable operation over a frequency range of 1–210 kHz with an output impedance of 0.0784 k Ω . The LF41 based amplifier showed linear performance up to 50 kHz, while the VCC produced stable injection currents ranging from 0.3 to 2 mA for load variations between 100 and 2000 Ω , with optimal stability at 10 kHz. Data acquisition using the adjacent method was performed on a 16-electrode phantom containing bovine bone as a resistive object. Image reconstruction using the iterative Newton Raphson method with Tikhonov regularization successfully identified the object's position and boundaries. The results demonstrate that the proposed system provides stable and reliable imaging suitable for medical EIT applications.

Keywords: current injection; data acquisition system; EIT; image reconstruction; medical imaging

1. Introduction

Electrical Impedance Tomography (EIT) is a non-invasive medical imaging technique that reconstructs the internal electrical resistivity distribution of an object by injecting low-amplitude alternating currents through surface electrodes and measuring the resulting boundary voltages [6], [7]. Due to its non-ionizing nature, low cost, and portability, EIT has gained increasing attention as an alternative imaging modality for continuous and bedside medical monitoring.

Recent studies have demonstrated the application of EIT in pulmonary monitoring, neurological assessment, and tissue characterization [1], [2], [5]. Advances in hardware design and signal processing have enabled EIT systems to provide clinically relevant information, particularly in respiratory monitoring during mechanical ventilation and weaning processes [2], [5]. Furthermore, optimization of electrode configurations and excitation parameters has been reported to significantly influence image quality and reconstruction accuracy [3], [4].

Despite these advantages, EIT images still suffer from limited spatial resolution due to measurement noise, instability of current injection, electrode contact impedance, and the ill-posed

nature of the inverse problem [8]. Therefore, the development of reliable hardware systems with stable current injection and accurate voltage measurement remains a critical research challenge.

This research focuses on the design and implementation of a 16-electrode EIT data acquisition system for medical imaging purposes. The proposed system emphasizes stable current injection, reliable voltage measurement, and effective image reconstruction. The novelty of this study lies in the development of a complete 16-electrode EIT hardware system with experimentally optimized current injection parameters (0.3 mA at 10 kHz), resulting in stable data acquisition and improved image reconstruction performance using a cost-effective design approach.

2. Materials and Methods

This study employed an experimental approach to design and evaluate a 16-electrode EIT data acquisition system. The developed hardware architecture consists of a sinusoidal signal generator based on the XR-2206 integrated circuit, an LF412-based amplifier, a voltage-to-current converter (VCC), an analog multiplexer/demultiplexer, and a microcontroller-based control unit. The excitation signal generated by the XR-2206 is amplified and converted into a constant current before being injected into the object under test. The overall hardware architecture of the proposed EIT data acquisition system is illustrated in Fig. 1.

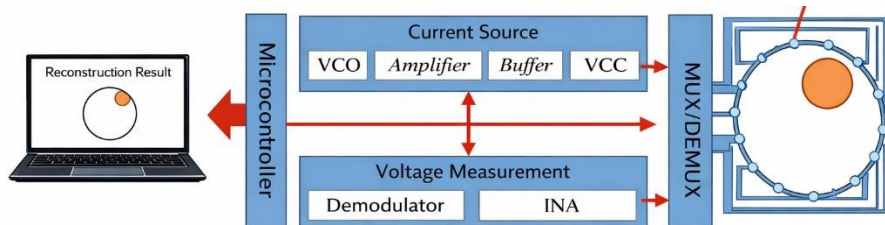


Figure 1 System block diagram of the proposed 16-electrode EIT data acquisition system

A cylindrical phantom filled with saline solution was used as the conductive medium, while bovine bone samples were placed inside the phantom to represent resistive inclusions, following experimental approaches reported in recent EIT studies [4]. The system employed the adjacent current injection and voltage measurement method, which is commonly adopted in practical EIT systems due to its simplicity and robustness [3], [9]. One complete measurement cycle produced 208 voltage data points. The electrode configuration and adjacent measurement pattern used in this study are shown in Fig. 2.

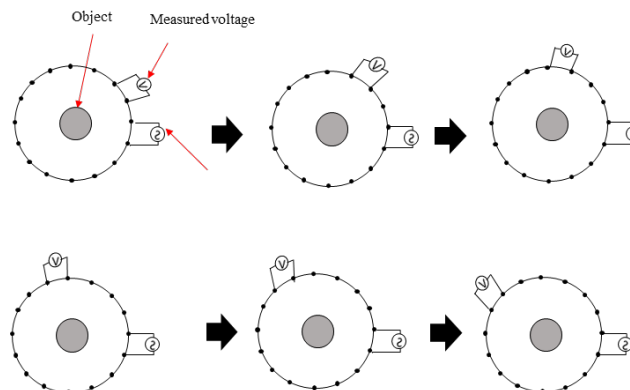


Figure 2 Electrode configuration and adjacent measurement pattern

Current injection levels ranging from 0.3 to 2 mA and excitation frequencies between 10 and 50 kHz were evaluated to determine optimal operating conditions. Acquired voltage data were transferred to a personal computer for post-processing. Image reconstruction was performed using an iterative Newton–Raphson algorithm combined with Tikhonov regularization to stabilize the

inverse problem and suppress noise effects [8], [9]. The reconstruction workflow is illustrated in Fig. 3. Initially, an estimated resistivity distribution was assigned to the imaging domain and discretized using a two-dimensional finite element method (2D FEM). Based on this initial estimate, boundary voltages were calculated by solving the forward problem under the same adjacent current injection pattern applied in the experimental measurements.

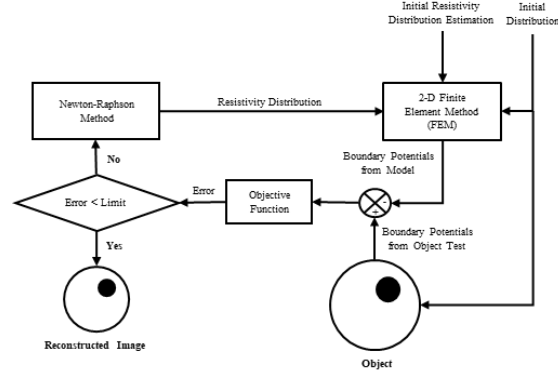


Figure 3 Block diagram of the iterative image reconstruction process using the Newton–Raphson algorithm

Initially, an estimated resistivity distribution was assigned to the imaging domain and discretized using a two-dimensional finite element method (2D FEM). Based on this initial estimate, boundary voltages were calculated by solving the forward problem under the same adjacent current injection pattern applied in the experimental measurements.

The inverse problem was formulated as an optimization problem by minimizing the discrepancy between the measured boundary voltages and the voltages calculated from the numerical model. The objective function is expressed as:

$$\Phi(\rho) = \|V_{meas} - V_{calc}(\rho)\|^2 \quad (1)$$

Where V_{meas} denotes the measured boundary voltage vector, V_{calc} represents the calculated voltage vector obtained from the FEM-based forward model, and ρ is the resistivity distribution. If the value of the objective function exceeded a predefined tolerance, the resistivity distribution was updated iteratively using the Newton–Raphson method with Tikhonov regularization. The update process can be expressed as:

$$\rho_{k+1} = \rho_k + \Delta\rho \quad (2)$$

Where ρ_k and ρ_{k+1} represent the resistivity distributions at the k -th and $(k+1)$ -th iterations, respectively, and $\Delta\rho$ is the correction term computed using the regularized Newton–Raphson formulation. The regularization term was incorporated to stabilize the solution and suppress noise amplification during the iterative process. The iteration was repeated until the error between the measured and simulated boundary voltages fell below the specified tolerance. The converged resistivity distribution was subsequently visualized as the final reconstructed EIT image.

3. Results

This section presents the experimental results obtained from the developed 16-electrode Electrical Impedance Tomography (EIT) system. The performance of the system is evaluated in terms of current injection stability, voltage measurement reliability, and image reconstruction capability. The effects of injection current amplitude and excitation frequency on boundary voltage measurements and reconstructed images are systematically analyzed.

3.1. Performance of the Current Injection System

The performance of the current injection subsystem was evaluated under varying frequency and load conditions. The XR-2206 signal generator produced a stable sinusoidal output voltage over a frequency range of 1–210 kHz, with an output impedance of approximately 0.0784 kΩ. As shown in Fig. 4, the XR-2206 generator exhibits stable output voltage and low output impedance across the evaluated frequency range.

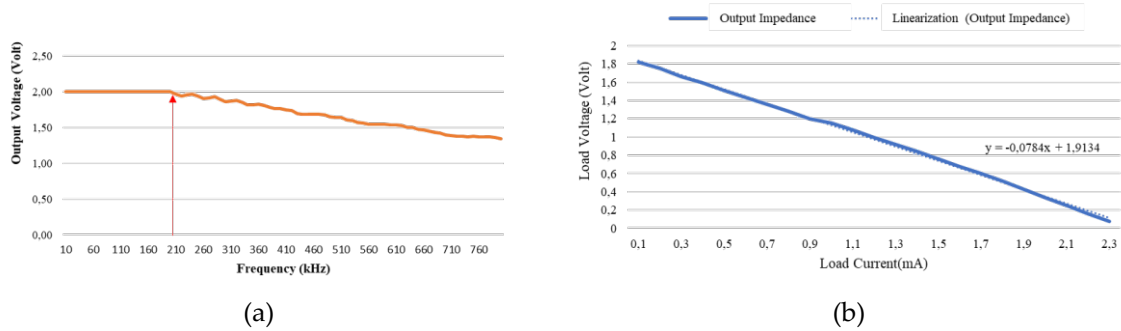


Figure 4 Performance characteristics of the XR-2206 signal generator: (a) output voltage stability as a function of excitation frequency, and (b) output impedance characterization

The voltage-controlled current source demonstrated stable current injection across load resistances ranging from 100 Ω to 2000 Ω, maintaining injected currents within 0.3–2 mA. The most stable operation was observed at an excitation frequency of 10 kHz, as illustrated in Fig. 5.

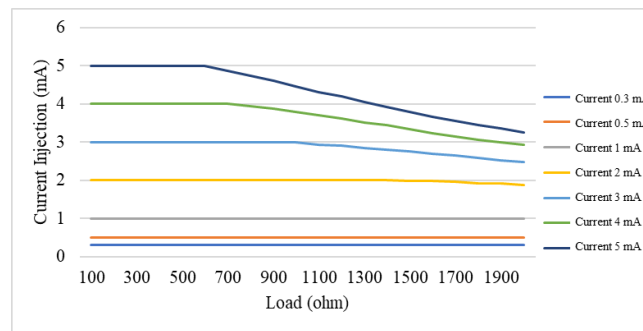


Figure 5 Current stability of the voltage-controlled current source under load variations

3.2. Voltage Measurement Results

Boundary voltage signals acquired from the phantom were characterized by low amplitudes in the millivolt range. After amplification using an instrumentation amplifier (AD620 Module) and RMS-to-DC conversion (IC AD536), the acquired signals exhibited a significant improvement in signal quality, as presented in Fig. 6.

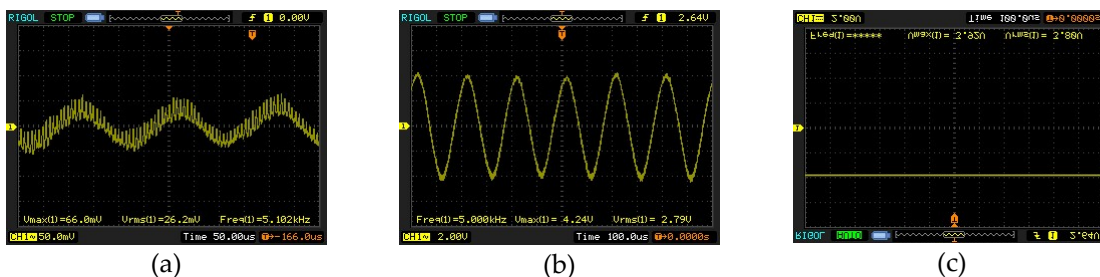


Figure 6 Boundary voltage signal processing stages: (a) raw electrode output signal, (b) output of the AD620 instrumentation amplifier with a gain of 64, and (c) output of the AD536 RMS-to-DC converter

Using the 16-electrode adjacent measurement protocol, the system successfully acquired 208 independent voltage measurements per acquisition cycle, demonstrating consistent and repeatable voltage patterns suitable for EIT image reconstruction

3.3. Effect of Injection Current Variation

The influence of injection current amplitude on voltage measurements was investigated using current levels of 0.3 mA, 0.5 mA, 1 mA, and 2 mA at a fixed excitation frequency of 10 kHz. The resulting voltage measurement profiles are presented in Fig. 7.

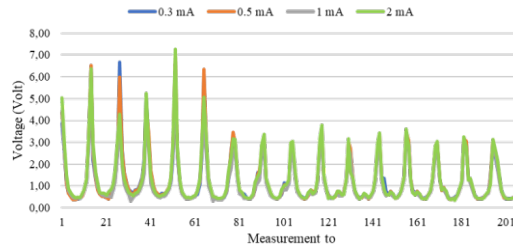


Figure 7 Voltage measurement profiles for different injection current levels

All tested current levels enabled detection of the resistive object within the phantom. Differences in signal amplitude and stability were observed across the tested current levels

3.4. Effect of Excitation Frequency Variation

The effect of excitation frequency on voltage measurements was evaluated at 10 kHz, 30 kHz, and 50 kHz, while maintaining a constant injection current of 0.3 mA. The corresponding voltage profiles are shown in Fig. 8.

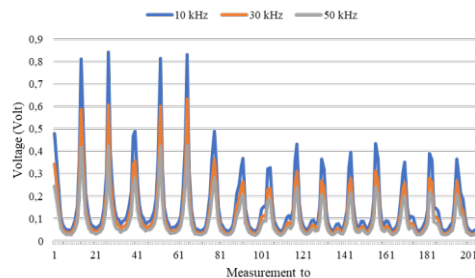


Figure 8 Voltage measurement profiles for different excitation frequencies

Variations in voltage contrast and spatial distribution were observed across the tested frequencies

3.5. Image Reconstruction Results

Reconstructed EIT images obtained under different excitation conditions are presented in Fig. 9 and Fig. 10. The reconstructed images reveal variations in object boundary clarity and spatial resolution depending on the applied current amplitude and excitation frequency.

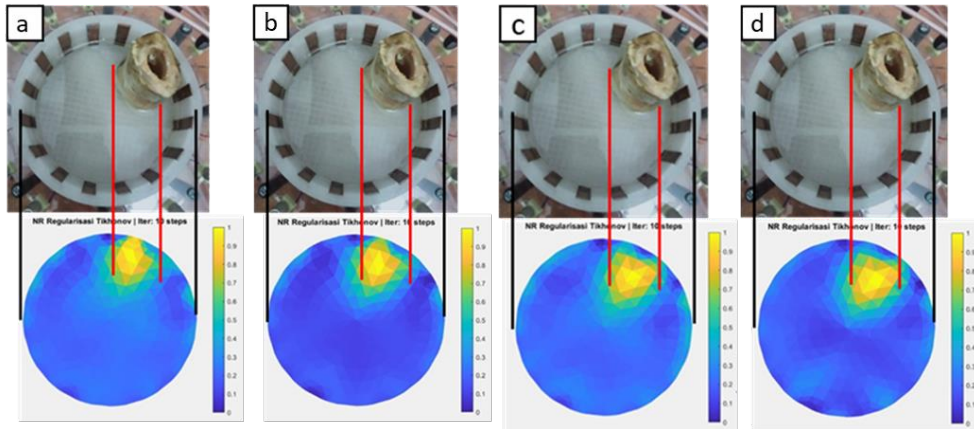


Figure 9 Reconstructed images for different injection current levels (a) 0,3 mA, (b) 0,5 mA, (c) 1 mA, and (d) 2 mA

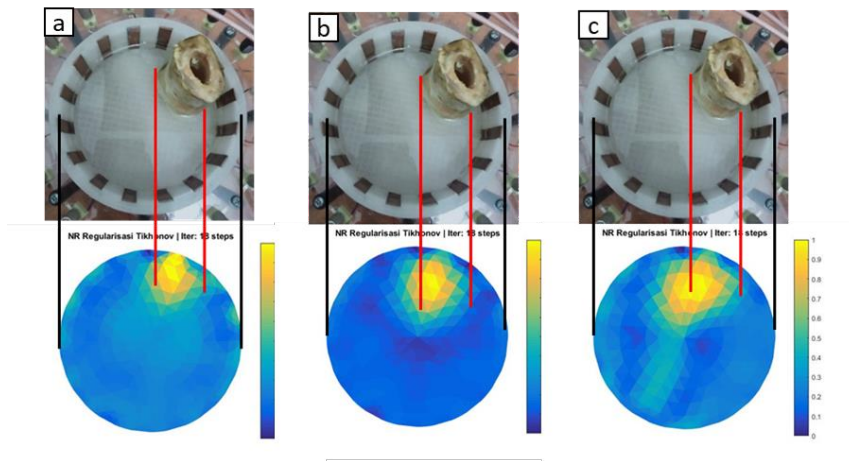


Figure 10 Reconstructed images for different excitation frequencies (a) 10 kHz, (b) 30 kHz, and (c) 50 kHz

The reconstruction result for two separated resistive objects, shown in Fig. 11, demonstrates the system's capability to distinguish multiple inclusions within the imaging domain.

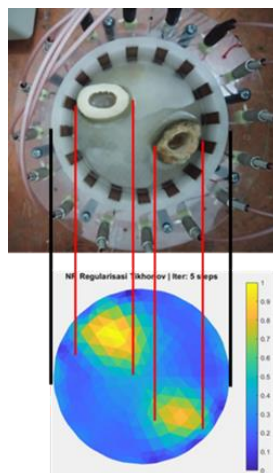


Figure 11 Reconstruction result for two separated resistive objects

4. Discussion

This section discusses the experimental results presented in the previous section by interpreting the observed trends and relating them to findings reported in recent EIT literature, with a focus on excitation stability, measurement reliability, and reconstruction performance of the proposed system. Despite the promising performance of the proposed 16-electrode EIT data acquisition system, several limitations should be acknowledged. The system performance may be affected by electrode contact impedance variations and electrical noise originating from analog components. Nevertheless, in comparison with previous EIT systems reported in the literature, the proposed design offers a simpler hardware configuration while maintaining comparable signal quality, making it suitable for low-cost medical imaging applications.

4.1. Current Injection and Measurement Stability

The stable output voltage of the XR-2206 signal generator and the consistent current injection achieved by the voltage-controlled current source indicate that the excitation subsystem meets the requirements for biomedical EIT applications. Stable current injection is critical, as fluctuations directly affect boundary voltage measurements and reconstruction accuracy. Similar observations have been reported in recent EIT system developments, where excitation stability was identified as a key factor influencing image quality [1], [2]

4.2. Influence of Injection Current Amplitude

Lower injection current amplitudes (0.3–1 mA) resulted in more stable voltage measurements compared to higher current levels. Although higher currents increased voltage amplitude, they also introduced increased variability. This behavior supports previous recommendations that low amplitude excitation provides an optimal balance between measurement stability, reconstruction accuracy, and safety considerations in medical EIT systems [3], [4]

4.3. Influence of Excitation Frequency

The results demonstrate that an excitation frequency of 10 kHz yields superior voltage contrast and improved image clarity compared to higher frequencies. This can be attributed to the frequency-dependent electrical properties of biological tissues, where resistive components dominate at lower frequencies. These findings are consistent with recent studies on frequency optimization in EIT-based tissue imaging [5], [9].

4.4. Image Reconstruction Performance

The reconstructed images confirm that the Newton–Raphson algorithm combined with Tikhonov regularization effectively stabilizes the ill-posed inverse problem inherent in EIT. The adjacent measurement strategy provides sufficient sensitivity for detecting resistive inclusions while maintaining a simple and robust hardware configuration. Although spatial resolution is limited by the number of electrodes, the obtained results demonstrate the feasibility of the proposed system for non-invasive imaging applications [10], [11].

The results confirm that stable current injection and accurate voltage measurement are critical factors influencing EIT image quality. Lower excitation frequencies contributed to improved signal stability and reduced sensitivity to measurement noise, in agreement with findings reported in recent EIT applications for medical monitoring [2], [5].

The Newton–Raphson reconstruction method combined with Tikhonov regularization effectively mitigated the ill-posed nature of the EIT inverse problem and improved image clarity. Although the spatial resolution remains lower than that of conventional imaging modalities, the proposed system demonstrates sufficient performance for non-invasive medical imaging research and experimental validation. The use of cost-effective electronic components further supports the feasibility of developing low-cost EIT systems for research and educational purposes, as suggested in recent EIT system development studies [3], [12].

5. Conclusions

This study aimed to design and implement a 16-electrode Electrical Impedance Tomography (EIT) data acquisition system for medical imaging applications. Experimental results demonstrate that the proposed system is capable of acquiring stable boundary voltage signals suitable for reliable image reconstruction. The developed system exhibited stable operation with current injection levels ranging from 0.3 to 2 mA and excitation frequencies up to 50 kHz. Optimal imaging performance was achieved at an injection current of 0.3 mA and a frequency of 10 kHz, resulting in improved spatial resolution and image contrast. Future work will focus on increasing the number of electrodes, enhancing noise reduction techniques, and implementing advanced image reconstruction algorithms to further improve imaging accuracy.

References

1. Y. Guo et al., "Electrical impedance tomography provides information of brain injury during total aortic arch replacement," *Scientific Reports*, vol. 14, art. 14236, 2024. DOI: <https://doi.org/10.1038/s41598-02465203-0>
2. J. J. Wisse et al., "Electrical impedance tomography as a monitoring tool during weaning from mechanical ventilation," *Respiratory Research*, vol. 25, art. 179, 2024. DOI: <https://doi.org/10.1186/s12931-024-02801-6>
3. A. Ramandha and Basari, "Performance optimization of electrode patterns in electrical impedance tomography," *Jurnal Informatika & Rekayasa Elektronik*, vol. 7, no. 2, pp. 210–217, 2024. DOI: <https://doi.org/10.36595/jire.v7i2.1224>
4. R. Aisya et al., "Application of electrical impedance tomography for detecting biological tissue," *Indonesian Journal of Electronics, Electromedical Engineering, and Medical Informatics*, vol. 7, no. 2, 2025. DOI: <https://doi.org/10.35882/ijeemi.v7i2.54>
5. Z. Cui et al., "Technical principles and clinical applications of electrical impedance tomography in pulmonary monitoring," *Sensors*, vol. 24, no. 14, art. 4539, 2024. DOI: <https://doi.org/10.3390/s24144539>
6. J. G. Webster, *Electrical Impedance Tomography*. Bristol, UK: Adam Hilger, 1990.
7. D. S. Holder, *Electrical Impedance Tomography: Methods, History and Applications*. London, UK: IOP Publishing, 2005.
8. B. H. Brown, "Electrical impedance tomography (EIT): A review," *Journal of Medical Engineering & Technology*, vol. 27, no. 3, pp. 97–108, 2003. DOI: <https://doi.org/10.1080/0309190021000059688>
9. A. Hassan, M. A. Rahman, and S. Ibrahim, "Performance evaluation of excitation current and frequency selection in electrical impedance tomography systems," *IEEE Access*, vol. 12, pp. 45621–45632, 2024. DOI: <https://doi.org/10.1109/ACCESS.2024.3372196>
10. M. Li, J. Sun, and X. Dong, "Improved image reconstruction in electrical impedance tomography using regularized Newton-based methods," *Measurement*, vol. 223, art. 113825, 2024. DOI: <https://doi.org/10.1016/j.measurement.2023.113825>
11. Y. Wang, Z. Cui, X. Li, and H. Zhang, "Design and implementation of a multi-channel electrical impedance tomography system for biomedical applications," *Biomedical Signal Processing and Control*, vol. 86, art. 105247, 2024. DOI: <https://doi.org/10.1016/j.bspc.2023.105247>
12. A. Adler and W. R. B. Lionheart, "Uses and abuses of EIDORS," *Physiological Measurement*, vol. 27, no. 5, pp. S25–S42, 2006. DOI: <https://doi.org/10.1088/0967-3334/27/5/S03>

